

Multi-Aspect Mining and Anomaly Detection for Heterogeneous Tensor Streams

Soshi Kakio

SANKEN, The University of Osaka
Osaka, Japan
sakio88@sanken.osaka-u.ac.jp

Ren Fujiwara

SANKEN, The University of Osaka
Osaka, Japan
r-fujiwr88@sanken.osaka-u.ac.jp

Yasuko Matsubara

SANKEN, The University of Osaka
Osaka, Japan
yasuko@sanken.osaka-u.ac.jp

Yasushi Sakurai

SANKEN, The University of Osaka
Osaka, Japan
yasushi@sanken.osaka-u.ac.jp

Abstract

Analysis and anomaly detection in event tensor streams consisting of timestamps and multiple attributes—such as communication logs (time, IP address, packet length)—are essential tasks in data mining. While existing tensor decomposition and anomaly detection methods provide useful insights, they face the following two limitations. (i) They cannot handle heterogeneous tensor streams, which comprises both categorical attributes (e.g., IP address) and continuous attributes (e.g., packet length). They typically require either discretizing continuous attributes or treating categorical attributes as continuous, both of which distort the underlying statistical properties of the data. Furthermore, incorrect assumptions about the distribution family of continuous attributes often degrade the model's performance. (ii) They discretize timestamps, failing to track the temporal dynamics of streams (e.g., trends, abnormal events), which makes them ineffective for detecting anomalies at the group level, referred to as "group anomalies" (e.g., DoS attacks). To address these challenges, we propose HETEROCOMP, a method for continuously summarizing heterogeneous tensor streams into "components" representing latent groups in each attribute and their temporal dynamics, and detecting group anomalies. Our method employs Gaussian process priors to model unknown distributions of continuous attributes, and temporal dynamics, which directly estimate probability densities from data. Extracted components give concise but effective summarization, enabling accurate group anomaly detection. Extensive experiments on real datasets demonstrate that HETEROCOMP outperforms the state-of-the-art algorithms for group anomaly detection accuracy, and its computational time does not depend on the data stream length.

CCS Concepts

- Information systems → Data stream mining; • Computing methodologies → Factorization methods.



This work is licensed under a Creative Commons Attribution 4.0 International License.
WWW '26, Dubai, United Arab Emirates
© 2026 Copyright held by the owner/author(s).
ACM ISBN 979-8-4007-2307-0/2026/04
<https://doi.org/10.1145/3774904.3792175>

Keywords

Bayesian tensor decomposition, Data stream, Anomaly detection, Gaussian process

ACM Reference Format:

Soshi Kakio, Yasuko Matsubara, Ren Fujiwara, and Yasushi Sakurai. 2026. Multi-Aspect Mining and Anomaly Detection for Heterogeneous Tensor Streams. In *Proceedings of the ACM Web Conference 2026 (WWW '26), April 13–17, 2026, Dubai, United Arab Emirates*. ACM, New York, NY, USA, 12 pages. <https://doi.org/10.1145/3774904.3792175>

1 Introduction

The rapid development of information systems has made it possible to obtain a variety of multi-aspect event data streams, which consist of a timestamp and multiple attributes (e.g., price, user ID, item name). Crucially, the effective analysis and anomaly detection of such streams have numerous real-world applications [27], including online marketing analytics [23], location-based services [11, 15, 29], and cybersecurity systems [3–5, 26, 41]. For example, marketers want to discover hidden groups of each attribute and their trends from user's review data. Furthermore, in cybersecurity systems, analyzing and detecting anomalies (e.g., DDoS attacks) from access logs as quickly as possible is crucial to minimize the damage from them. Since there is no anomaly label in streaming settings, in this work, we focus on the analysis and unsupervised anomaly detection of multi-aspect data streams.

These multi-aspect data streams are represented as high dimensional tensor streams, which are inherently sparse [27], where the number of present records is much smaller than the tensor size. Despite the wide success of existing tensor decomposition algorithms [16], which aim to reveal hidden structures and relationships of tensors, this sparsity derails typical tensor decomposition methods because they are designed for dense tensors. Recent studies focused on the streaming decomposition of sparse tensors [11, 15, 17, 55], with an effective strategy being the components-based methods [23, 26, 27] that capture hidden groups in each attribute and their relationships. However, most existing methods can handle only categorical attributes (e.g., IP address, port, user ID), and cannot handle continuous attributes (e.g., price, flow duration, packet size). Here, we refer to such tensor streams that consist of both categorical attributes and continuous attributes as *heterogeneous tensor stream*. To handle heterogeneous tensor streams, existing methods require discretizing continuous attributes, which disrupts the continuity

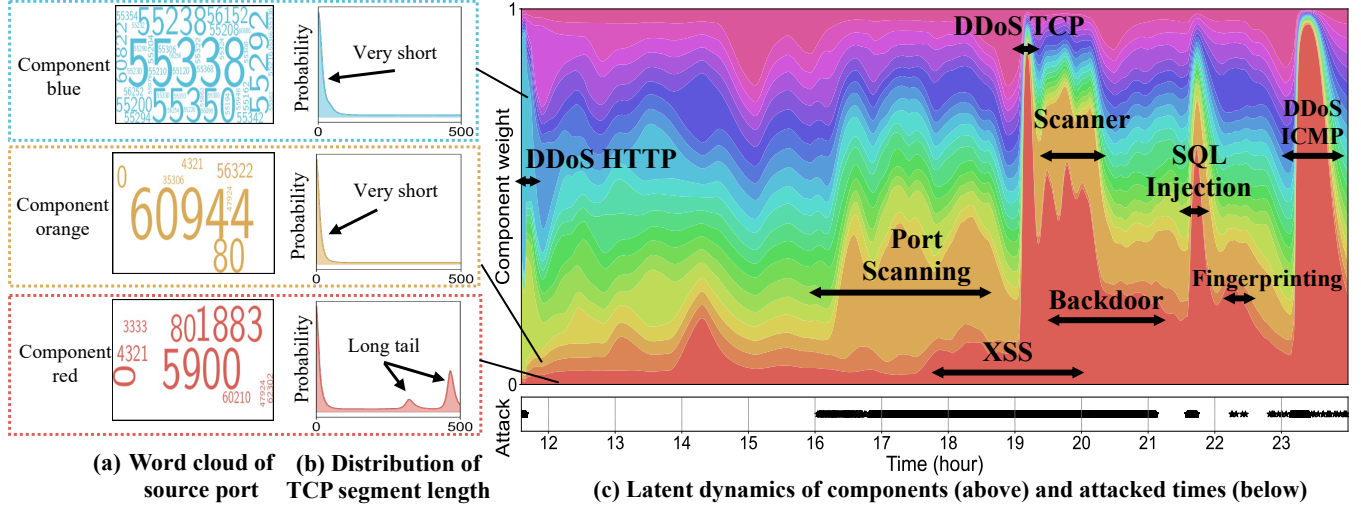


Figure 1: Modeling power of HETEROCOMP over (#3) Edge-IIoT dataset. Our proposed method can find the hidden components which represents different characteristics in both (a) categorical attribute (source port) and (b) continuous attribute (TCP segment length), and (c) component weight exhibit significant changes when cyber-attacks occurs.

of continuous attributes. Furthermore, in real-world scenarios, we often have no information about the continuous attributes; that is, we do not know the distributions of continuous attributes. Incorrect assumptions about the distribution family often degrade the model's performance.

Typical streaming unsupervised anomaly detection methods [6, 10, 22] are effective at identifying anomalous records (*point anomalies*). However, as they ignore the temporal relationships between records, they cannot effectively detect *group anomalies* (also referred to as collective anomalies), which may not be anomalies by themselves, but their occurrence together as a collection exhibits unusual patterns that deviate from the entire data set [8]. A canonical example of group anomalies is a DoS attack: an individual request could possibly be normal, but their high-frequency aggregation over a short duration constitutes a critical threat. Although methods for detecting group anomalies [5, 41, 53] have been developed, they cannot handle heterogeneous tensor streams; they enforce data homogeneity by either discretizing continuous attributes or treating categorical attributes as continuous, both of which distort the underlying statistical properties of the data. Furthermore, by discretizing timestamps, they fail to preserve their continuity. In summary of the above discussion, we wish to solve the following problem: *Given a heterogeneous tensor stream, how can we find hidden structures of the stream without restricting to any specific parameterized form of continuous attributes, and quickly and accurately detect group anomalies?*

In this paper, to tackle the above challenging problems, we propose HETEROCOMP¹, for continuously summarizing heterogeneous tensor streams into components and their temporal dynamics, and detect group anomalies based on the components without restricting to any specific parameterized form. Specifically, to model the unknown distribution of continuous attributes, HETEROCOMP uses

logistic Gaussian process priors [35], which directly estimate probability densities from data, thus HETEROCOMP can treat continuous attributes uniformly. In addition, HETEROCOMP models the components' latent dynamics using the Gaussian process, which utilizes the continuity of timestamps and captures complex temporal evolutions(changes) of components linked to external events. Extracted components naturally represent latent groups in both categorical and continuous attributes, and relationship between attributes, which provide an easy-to-understand summary of data. Similar records tend to cluster into the same component, which enables accurate group anomaly detection by aggregating abnormal records. The framework further admits streaming updates without retraining from scratch, making it suitable for long-running deployments where heterogeneous tensor streams arrive continuously, and enabling low computational cost incorporation of new records.

1.1 Preview of Our Result

Fig. 1 shows an example of the analysis of heterogeneous tensor stream (i.e., (#3) Edge-IIoT) using HETEROCOMP. This dataset consists of records with categorical attributes, continuous attributes, and timestamps. Our method captures the following properties:

- **Modeling Heterogeneity:** Fig. 1(a)(b) shows the characteristics of three components blue, orange, and red. First, Fig. 1(a) shows the word clouds of source port attribute. A larger size in the word cloud denote a stronger relationship with the component. Component blue is associated with records sent from ports 55338 and 55350 whereas component orange is dominated by records on port 60944, and component Red have records sent from ports 5900 and 1883. Next, Fig. 1(b) shows the distribution of the length of the TCP segment attribute. Component blue and orange encompass records featuring short TCP segments, while component red primarily represents records with long TCP segments.
- **Latent Dynamics:** Fig. 1(c) visualizes the latent dynamics of components, where the area of each color represents the component assignment probability at each time. The dynamics of

¹Our source code is publicly available in <https://github.com/kaki005/HeteroComp>.

Table 1: Capabilities of approaches.

	RRCF[10]	MStream[3]	MemStream[4]	Anograph[5]	Trimine[23]	CubeScope[27]	CyberCScope[26]	HETEROCOMP
Anomaly detection	✓	✓	✓	✓	-	✓	✓	✓
Multi-aspect mining	-	-	-	-	✓	✓	✓	✓
Stream processing	✓	✓	✓	✓	-	✓	✓	✓
Heterogeneous	-	✓	-	-	-	-	✓	✓
Latent dynamics	-	-	-	-	-	-	-	✓

these latent components exhibit significant changes when cyber-attacks occurs. Specifically, component blue becomes dominant over others when a DDoS HTTP attack occurs, while component orange becomes dominant during an attack originating from a different source port, such as Port Scanning and Vulnerability Scanner. Similarly, component red tends to increase during attacks characterized by the transmission of many packets with large TCP segment sizes, such as DDoS TCP, DDoS ICMP.

Contributions. In this paper, we propose HETEROCOMP, which has the following desirable properties:

- *Effective*: Our proposed model summarizes heterogeneous tensor streams without restricting to any specific parameterized form, which extracts interpretable latent components and their latent dynamic (i.e., Fig. 1).
- *Accurate*: Extensive experiments on real-world datasets shows that HETEROCOMP outperforms baseline approaches for detecting group anomalies accurately.
- *Scalable*: Our proposed algorithm is fast and its computation time does not depend on the entire stream length.

2 Related Work

In this section, we briefly describe investigations related to this research. Table 1 shows the relative advantages of our method, and only HETEROCOMP meets all the requirements.

Sparse Tensor Decomposition. A wide range of studies have been conducted on analyzing sparse tensors, including probabilistic generative models[23, 37, 44, 46, 47, 54] and neural-based models[1]. In particular, streaming algorithms have become more critical in terms of processing a substantial amount of data under time/memory limitations, and they have proved highly significant to the data mining and database community [7, 17, 42, 55]. CubeScope [27] can summarize an event tensor stream interpretably, such as distinct patterns that change over time or major trends in categorical attributes. However, they can handle only categorical attributes, so they enforce data homogeneity by discretizing continuous attributes, which disrupts the continuity of continuous attributes. Only CyberCScope [26] can handle heterogeneous tensor streams by distinguishing between categorical attributes and continuous attributes, but it only supports the case where the continuous attributes follow Gamma distributions, which may diminish component diversity. Furthermore, it uses Multinomial distribution to

model component evolution over time, failing to capture complex dynamics.

Streaming Anomaly Detection. Over decades, popular anomaly detection methods have been extended to work online on a data stream[25, 30, 36, 50, 52], including One Class SVM [38], isolation forest [6, 10], and deep learning methods [51]. However, they are designed for point anomaly detection, failing to detect group anomalies. Although MemStream [4] can handle the time-varying data distribution known as concept drift [21] and robust to group anomalies, it cannot handle categorical attributes. Recent methods for group anomaly detection of multi-aspect data stream are mainly categorized into graph-based methods[2, 5, 8] which aim to detect node/edge/graph anomalies in graph streams, and tensor-based methods [14, 41, 53] which aim to detect suddenly appearing dense subtensors in sparse tensor streams. However, they are designed for categorical attributes, failing to handle heterogeneous tensor streams. Although Mstream [3] can detect group anomalies from multi-aspect data involving categorical and continuous attributes, it discretizes timestamps, which degrades detection accuracy. Furthermore, they cannot summarize the streams interpretably.

Deep Generative Models. Although many deep generative models have been proposed to model heterogeneous tabular data[28, 48] and non-parametric distributions [34], they are computationally expensive for streaming scenarios.

3 Proposed Method

3.1 Problem Settings

We continuously monitor a stream of records $\{\mathbf{e}_1, \mathbf{e}_2, \dots\}$, arriving in a streaming manner. Each record \mathbf{e}_i consists of timestamps τ_i , M_1 categorical attributes $\{e_i^{(m_1)}\}_{m_1=1}^{M_1}$, and M_2 continuous attributes $\{e_i^{(m_2)}\}_{m_2=1}^{M_2}$. For the m_1 -th categorical attribute, we assume a finite U_{m_1} -th dimensional space, whereas for the m_2 -th continuous attribute, we assume a real space \mathbb{R} . This stream takes the form of a $(1 + M_1 + M_2)$ -th order tensor $\mathcal{X} \in \mathbb{N}^{T \times \prod_{m_1=1}^{M_1} U_{m_1} \times \prod_{m_2=1}^{M_2} \mathbb{R}}$, where T is the number of timestamps up to the current time. For each of the non-overlapping $T_c \ll T$ timestamps, we can obtain $\mathcal{X}^C \in \mathbb{N}^{T_c \times \prod_{m_1=1}^{M_1} U_{m_1} \times \prod_{m_2=1}^{M_2} \mathbb{R}}$ as the partial tensor of \mathcal{X} . Our goal is to summarize continuously growing \mathcal{X} and detect group anomalies by processing it incrementally as subtensor \mathcal{X}^C .

3.2 Gaussian Process

To model the latent dynamics of component and the distribution of continuous attributes, we use Gaussian processes [33], which are distributions over functions, fully specified by a kernel covariance function κ , such that any finite set of function values is jointly Gaussian. Specifically, for a finite set of inputs $X = \{x_1, \dots, x_n\}$, the function values are distributed as

$$f \sim GP(0, \kappa) \stackrel{\text{def}}{\iff} (f(x_1), \dots, f(x_n)) \sim \text{Normal}(\mathbf{0}, \mathbf{K}), \quad (1)$$

where $\mathbf{K}_{i,j} = \kappa(x_i, x_j)$ is a covariance matrix.

3.3 Model

We now present our model in detail. We assume that there are K major trends behind the event collections and refer to such trends

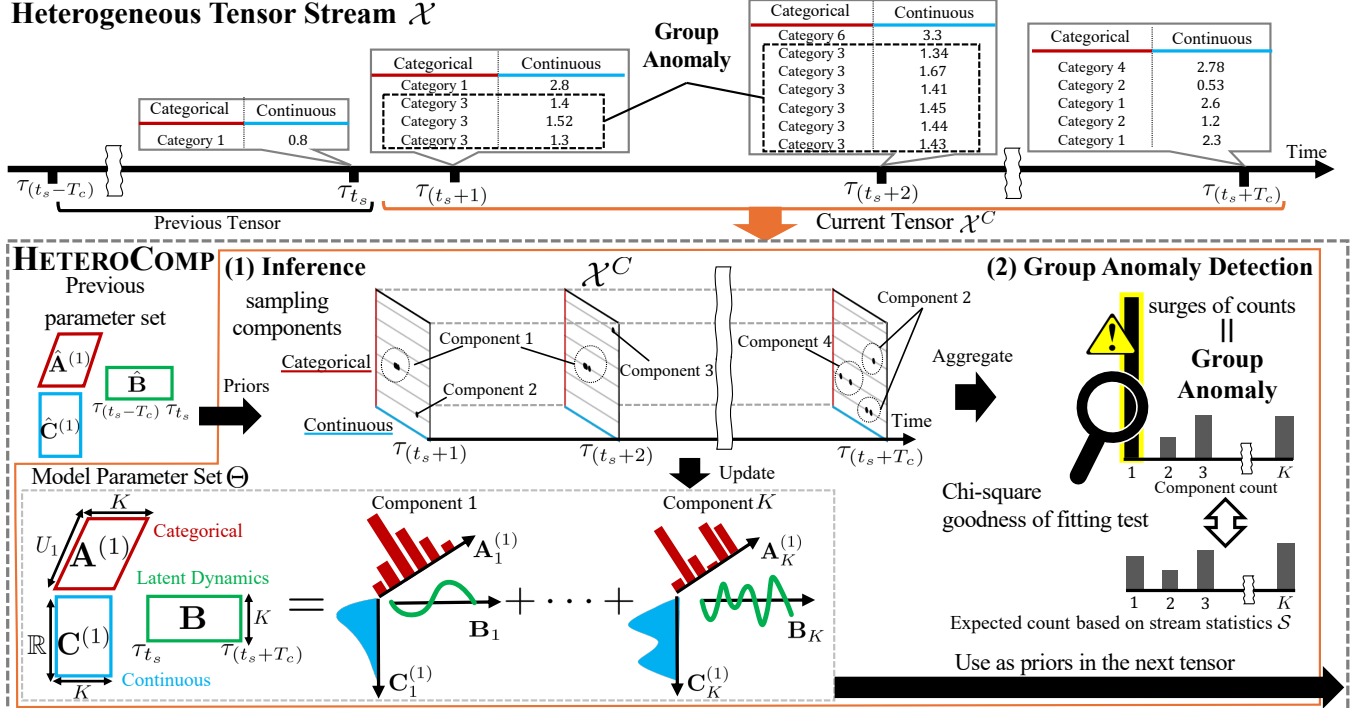


Figure 2: Illustration of HETEROCOMP: Given a current tensor X^C consisting one categorical attribute and one continuous attribute, (1) it assigns components to each record in X^C and update model parameter $A^{(1)}, C^{(1)}, B$, (2) it quickly and accurately detects group anomalies based on components counts.

as “component”. As shown in Fig. 2, the k -th component is characterized by the following probability distributions.

- $A_k^{(m_1)} \in \mathbb{R}^{U_{m_1}}$: Multinomial distribution over the m_1 -th categorical attribute, for the component k .
- $B_k \in \mathbb{R}^{T_c}$: Latent dynamics for the component k .

$$B_k \sim GP(0, \kappa_B). \quad (2)$$

- $C_k^{(m_2)} \in \mathbb{R}^{G_{m_2}}$: Distribution for m_2 -th continuous attribute, the component k . To model an unknown distribution in \mathbb{R} , we use a logistic Gaussian process (LGP) prior:

$$C_k^{(m_2)} \sim GP(0, \kappa_C), \quad (3)$$

$$p_{LGP}(e^{(m_2)} \in \Delta_g^{(m_2)}) = \frac{\exp(C_k^{(m_2)}(e^{(m_2)}))}{\int_{\mathbb{R}} \exp(C_k^{(m_2)}(e')) de'}. \quad (4)$$

We discretize \mathbb{R} into G_{m_2} non-overlapping grids $\{\Delta_g^{(m_2)}\}_{g=1}^{G_{m_2}}$ to improve the efficiency of inference. In other words, we use the following probability distribution instead of Eq. (4) :

$$p_{LGP}(e^{(m_2)} \in \Delta_g^{(m_2)}) \approx \frac{|\Delta_g^{(m_2)}| \exp(c_{k,g}^{(m_2)})}{\sum_{g'=1}^{G_{m_2}} |\Delta_{g'}^{(m_2)}| \exp(c_{k,g'}^{(m_2)}), \quad (5)}$$

where $|\Delta_g^{(m_2)}|$ is the width of the g -th grid, and $c_{k,g}^{(m_2)}$ is a predicted value at the center point of $\Delta_g^{(m_2)}$.

DEFINITION 1 (MODEL PARAMETER SET: Θ). Let $\Theta = \{ \{A^{(m_1)}\}_{m_1=1}^{M_1}, B, \{C^{(m_2)}\}_{m_2=1}^{M_2} \}$ be a parameter set of HETEROCOMP in X^C .

We also incorporate temporal dependencies into this model so that each parameter captures the context of its predecessors in the data stream. Specifically, we assume that the means of A, C are the same as \hat{A}, \hat{C} , which are the parameters estimated at the previous tensor, unless the newly arrived tensor X^C are confirmed. With this assumption, we can use Dirichlet($\alpha^{(m_1)} \hat{A}_k$) for categorical attributes, and Normal($\hat{C}_k^{(m_2)}, \sigma_C^2 I$) for continuous attributes. $\alpha^{(m_1)}$ is a hyperparameter representing the temporal persistence of the m_1 -th categorical attribute.² Consequently, as shown in the graphical model in Fig. 3, the generative process of X^C can be described as follows:

- For each component $k = 1, \dots, K$:
 - For each categorical attribute $m_1 = 1, \dots, M_1$:
 - * $A_k^{(m_1)} \sim \text{Dirichlet}(\alpha^{(m_1)} \hat{A}_k^{(m_1)})$
 - For each continuous attribute $m_2 = 1, \dots, M_2$:
 - * $C_k^{(m_2)} \sim \text{Normal}(\hat{C}_k^{(m_2)}, \sigma_C^2 I)$
- For each time $t = t_s + 1, \dots, t_s + T_c$:
 - For each record $n = 1, \dots, N_t$:
 - * $z_{t,n} \sim \text{Categorical}(\text{softmax}(B_t))$ // Component.
 - * For each categorical attribute $m_1 = 1, \dots, M_1$:
 - $e_{t,n}^{(m_1)} \sim \text{Categorical}(A_{z_{t,n}}^{(m_1)})$
 - * For each continuous attribute $m_2 = 1, \dots, M_2$:
 - $e_{t,n}^{(m_2)} \sim p_{LGP}(e_{t,n}^{(m_2)} | C_{z_{t,n}}^{(m_2)})$ // Eq.(5)

where N_t is the total number of records at time t , and $z_{t,n}$ is the component assignment. We note that the benefits of this model

²We set $\alpha^{(m_1)} = \frac{1}{K}$ as default.

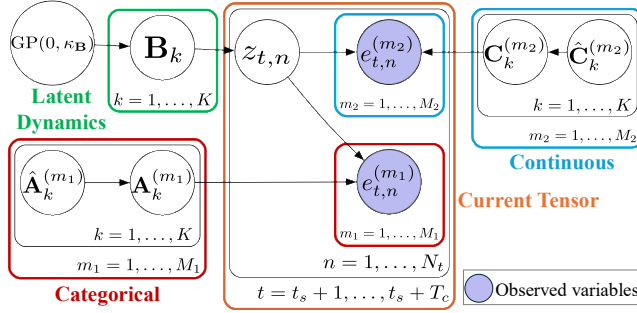


Figure 3: Graphical model of HETEROComp.

are three-fold. First, our model can summarize arbitrary-order heterogeneous sparse tensors into K components. Second, our model employs Gaussian process for B and C , enabling unified handling of continuous attributes and capturing complex dynamics of components. Lastly, to capture temporal dependencies, it employs the parameters of the previous tensor rather than storing tensors.

4 Algorithm

Before turning to the main topic, we introduce statistics for anomaly detection.

DEFINITION 2 (STREAM STATISTICS: \mathcal{S}). Let $\mathcal{S} = \{\mathcal{T}, \mathbf{S}^{(K)}, \{\mathbf{S}^{(m1)}\}_{m1=1}^{M1}, \{\mathbf{S}^{(m2)}\}_{m2=1}^{M2}\}$ be a statistics set of the entire stream \mathcal{X} . \mathcal{T} is the total normal time, and $\mathbf{S}^{(K)} \in \mathbb{N}^K$ is the total component count vector of normal records. $\mathbf{S}^{(m1)} \in \mathbb{N}^{K \times U_{m1}}$ and $\mathbf{S}^{(m2)} \in \mathbb{N}^{K \times G_{m2}}$ denote the total component-unit and component-grid count matrices of normal records, respectively.

With the above definitions, the formal problem is as follows:

PROBLEM 1. Given the current tensor \mathcal{X}^C as a partial tensor of \mathcal{X} ,

- Estimate the model parameter set Θ ,
- Maintain the stream statistics \mathcal{S} of \mathcal{X} ,
- Report the anomaly score for \mathcal{X}^C ,

incrementally and quickly, at any point in time.

In this section, we present practical algorithms for solving Problem 1. Algorithm 1 shows the overall procedure. Specifically, we first infer the component assignments and model parameter set Θ from \mathcal{X}^C , and then calculate the anomaly score of \mathcal{X}^C .

4.1 Inference

According to the generative process, we efficiently estimate parameters by employing collapsed Gibbs sampling [32]. Specifically, we repeatedly estimate B and sample components of each record, and then estimate A and C after the components have converged.

Sampling components. We sample components for each record in \mathcal{X}^C according to the following probability:

$$p(z_{t,n} = k | \cdot) \propto \text{softmax}(\mathbf{B}(\tau_n))_k \times \prod_{m1=1}^{M1} \frac{\mathbf{N}_{k, e_{t,n}^{(m1)}}' + \alpha^{(m1)} \hat{\mathbf{A}}_{k, e_{t,n}^{(m1)}}}{\mathbf{N}_k^{(K)'} + \alpha^{(m1)}} \prod_{m2=1}^{M2} p_{LGP}(e_{t,n}^{(m2)} | \mathbf{C}_k^{(m2)}), \quad (6)$$

where $\mathbf{N}_k^{(K)}$ is the number of records assigned to component k and $\mathbf{N}_{k,u}^{(m1)}$ is the total counts component k is assigned to the u -th unit.

Algorithm 1 HETEROComp (\mathcal{X}^C, Θ)

Input: 1. Current tensor: $\mathcal{X}^C \in \mathbb{N}^{T_c \times \prod_{m1=1}^{M1} U_{m1} \times \prod_{m2=1}^{M2} \mathbb{R}}$
2. Previous model parameter set: $\hat{\Theta}$
3. Previous stream statistics: \mathcal{S}

Output: 1. Updated model parameter set: Θ
2. Updated stream statistics: \mathcal{S}
3. Anomaly score: $\text{score}(\mathcal{X}^C)$

```

1: /* Inference */
2: for each iteration do
3:   for each record in  $\mathcal{X}^C$  do
4:     Draw component  $z_{t,n}$  // Eq. (6)
5:   end for
6:   for  $k = 1, \dots, K$  do
7:     for  $t = t_s + 1, \dots, t_s + T_c$  do
8:       Draw polya gamma  $\omega_{t,k}$  // Eq. (7)
9:       Caluculate  $(\mu_{t,k})_{pg}, (\sigma_{t,k}^2)_{pg}$  // Eq.(9),(10)
10:    end for
11:    Estimate  $\mathbf{B}_k$  // Eq.(16) - (23)
12:  end for
13: end for
14: Estimate  $\{\mathbf{A}^{(m1)}\}_{m1=1}^{M1}, \{\mathbf{C}^{(m2)}\}_{m2=1}^{M2}$  // Eq. (26), (24)
15:  $\Theta \leftarrow (\{\mathbf{A}^{(m1)}\}_{m1=1}^{M1}, \mathbf{B}, \{\mathbf{C}^{(m2)}\}_{m2=1}^{M2})$ 
16: /* Group Anomaly Detection */
17: Calculate  $\text{score}(\mathcal{X}^C)$  and p-value // Eq. (30)
18: if p-value < 0.05 then
19:   Report anomaly
20: else
21:   Add  $\delta_c, \mathbf{N}^{(K)}, \{\mathbf{N}^{(m1)}\}_{m1=1}^{M1}, \{\mathbf{N}^{(m2)}\}_{m2=1}^{M2}$  to  $\mathcal{S}$ 
22: end if
23: return  $\Theta, \mathcal{S}, \text{score}(\mathcal{X}^C)$ 

```

The prime (e.g., $\mathbf{N}_k^{(K)'} \mathbf{N}_k^{(K)''}$) indicates the count yielded by excluding the record $e_{t,n}$.

Estimate B. After sampling components, we estimate the posterior distribution of B based on the sampled components. However, we cannot directly use Gibbs sampling because a softmax function is non-conjugate. To address this, we used the Polya-Gamma data augmentation trick [31] to conjugate the softmax function. First, for each component and for each time, we sample $\omega_{t,k}$ according to the following equation:

$$\omega_{t,k} \sim \text{PolyaGamma}(N_{t,k}, \mu_{t,k} - \xi_{t,k}), \quad (7)$$

$$\xi_{t,k} = \log \sum_{j \neq k} e^{\mu_{j,t}}, \quad (8)$$

where $\mu_{t,k}$ is prior mean of $\mathbf{B}_k(\tau_t)$ and $N_{t,k}$ is the number of records assigned to the component k at time τ_t . Then, we compute posterior mean $(\mu_{t,k})_{pg}$ and variance $(\sigma_{t,k}^2)_{pg}$.

$$(\sigma_{t,k}^2)_{pg} = \left((\sigma_{t,k}^2)^{-1} + \omega_{t,k} \right)^{-1}, \quad (9)$$

$$(\mu_{t,k})_{pg} = (\sigma_{t,k}^2)_{pg} \left((\sigma_{t,k}^2)^{-1} \mu_{t,k} + N_{t,k} - \frac{N_t}{2} + \omega_{t,k} \xi_{t,k} \right), \quad (10)$$

where $\sigma_{t,k}^2$ is the prior variance of $\mathbf{B}_k(\tau_t)$.

Next, we perform Gaussian process regression for $\{(\mu_{t,k})_{pg}\}_{t=t_s+1}^{t_s+T_c}$ to estimate the posterior of \mathbf{B}_k . However, naive computation takes $O(T_c^3)$ time, so we approximate \mathbf{B}_k as a linear time-invariant stochastic differential equation (LTI-SDE):

$$\mathbf{x}_k(t) = \left(\mathbf{B}_k(t), \frac{d\mathbf{B}_k(t)}{dt}, \dots, \frac{d^p \mathbf{B}_k(t)}{dt^p} \right), \quad (11)$$

$$\mathbf{B}_k(t) = \mathbf{Hx}_k(t) + \epsilon_t \quad (\epsilon_t \sim \text{Normal}(0, \sigma_{noise}^2)), \quad (12)$$

$$\frac{d\mathbf{x}_k(t)}{dt} = \mathbf{Fx}_k(t) + \mathbf{Lw}(t), \quad (13)$$

where p is the order of the derivative, $\mathbf{w}(t) \in \mathbb{R}^s$ is a multivariate white noise process with a spectral density matrix $\mathbf{Q}_{noise} \in \mathbb{R}^{s \times s}$, and $\mathbf{F} \in \mathbb{R}^{(p+1) \times (p+1)}$, $\mathbf{L} \in \mathbb{R}^{(p+1) \times s}$, $\mathbf{H} \in \mathbb{R}^{1 \times (p+1)}$ is a feedback, a noise effect, and an observation matrix. Many covariance functions can be expressed as (13) equivalently or approximately [43]. For discrete values, this translates into

$$\mathbf{x}_k(\tau_t) = \Phi_{t-1}\mathbf{x}_k(\tau_{t-1}) + \mathbf{q}_{t-1}, \quad \mathbf{q}_{t-1} \sim \text{Normal}(\mathbf{0}, \mathbf{Q}_{t-1}), \quad (14)$$

$$\Phi_{t-1} = e^{\mathbf{F}(\tau_t - \tau_{t-1})}, \quad \mathbf{Q}_{t-1} = \mathbf{P}_\infty - \Phi_{t-1}\mathbf{P}_\infty\Phi_{t-1}^T.$$

The initial state is distributed according to $\mathbf{x}_k(\tau_{t_s}) \sim \text{Normal}(\mathbf{m}_{k,t_s}^s, \mathbf{P}_{k,t_s}^s)$, where $\mathbf{m}_{k,t_s}^s, \mathbf{P}_{k,t_s}^s$ are the posterior parameters in the previous tensor, computed according to Eq. (22), (23)³. Stationary covariance \mathbf{P}_∞ can be found by solving the Lyapunov equation:

$$\mathbf{FP}_\infty + \mathbf{P}_\infty\mathbf{F}^T + \mathbf{LQ}_{noise}\mathbf{L}^T = \mathbf{0}. \quad (15)$$

By approximating the Gaussian process regression as in Eq. (14), the regression problem can be solved with $O(T_c p^3)$ time complexity and $O(T_c p^2)$ memory complexity using a Kalman filter and a Rauch-Tung-Striebel (RTS) smoother. Specifically, the forward filtering update formula is obtained as follows:

$$\mathbf{m}_{k,t}^p = \Phi_{t-1}\mathbf{m}_{k,t-1}^f, \quad (16)$$

$$\mathbf{P}_{k,t}^p = \Phi_{t-1}\mathbf{P}_{k,t-1}^f\Phi_{t-1}^T + \mathbf{Q}_{t-1}, \quad (17)$$

$$\mathbf{R}_{k,t} = \mathbf{P}_{k,t}^p\mathbf{H}^T(\sigma_{t,k}^2)^{-1}, \quad (18)$$

$$\mathbf{m}_{k,t}^f = \mathbf{m}_{k,t}^p + \mathbf{R}_{k,t}((\mu_{t,k})_{pg} - \mathbf{H}\mathbf{m}_{k,t}^p), \quad (19)$$

$$\mathbf{P}_{k,t}^f = (\mathbf{I} - \mathbf{R}_{k,t})\mathbf{P}_{k,t}^p, \quad (20)$$

where $\mathbf{m}_{k,t}^p, \mathbf{P}_{k,t}^p$ is a predicted mean and covariance of $\mathbf{x}_k(\tau_t)$. Furthermore, the backward smoothing update formula is also obtained as follows:

$$\mathbf{J}_{k,t} = \mathbf{P}_{k,t}^f\Phi_{t-1}^T(\mathbf{P}_{k,t+1}^p)^{-1}, \quad (21)$$

$$\mathbf{m}_{k,t}^s = \mathbf{m}_{k,t}^f + \mathbf{J}_{k,t}(\mathbf{m}_{k,t+1}^s - \Phi_{t-1}\mathbf{m}_{k,t}^f), \quad (22)$$

$$\mathbf{P}_{k,t}^s = \mathbf{P}_{k,t}^f + \mathbf{J}_{k,t}(\mathbf{P}_{k,t+1}^s - \mathbf{P}_{k,t}^p)\mathbf{J}_{k,t}^T, \quad (23)$$

where $\mathbf{m}_{k,t}^s, \mathbf{P}_{k,t}^s$ is a smoothed mean and covariance of $\mathbf{x}_k(\tau_t)$. To summarize, we use $\text{Normal}(\mathbf{m}_{k,t}^p, \mathbf{P}_{k,t}^p)$ as the distribution for $\mathbf{x}_k(\tau_t)$ in the first epoch, and $\text{Normal}(\mathbf{m}_{k,t}^s, \mathbf{P}_{k,t}^s)$ in subsequent epochs.

Estimate A. After Gibbs sampling has burned in, we compute the posterior of A. Because the Dirichlet distribution is conjugate to the Categorical distribution, we can compute A analytically, as follows:

$$\mathbf{A}_{k,u}^{(m_1)} = \frac{\mathbf{N}_{k,u}^{(m_1)} + \alpha^{(m_1)}\hat{\mathbf{A}}_{k,u}^{(m_1)}}{\mathbf{N}_k^{(K)} + \alpha^{(m_1)}}, \quad (24)$$

where $\mathbf{N}_{k,u}^{(m_1)}$ is the total count of component k that is assigned to the u -th unit in the m_1 -th categorical attribute.

Estimate C. After Gibbs sampling has burned in, we compute the posterior of C. For convenience, we denote $|\Delta_g^{(m_2)}|$ as w_g . First, we approximate C as LTI-SDE, similar to B. Next, to estimate the

³We employ $\mathbf{m}_{k,t_s}^f = \mathbf{0}$ and $\mathbf{P}_{k,t_s}^f = \mathbf{P}_0$ at the first tensor.

unknown density, we use MAP estimation, which aims to find \mathbf{c}_k that maximizes the following log-likelihood:

$$L(\mathbf{c}_k) = \sum_{g=1}^{G_{m_2}} \mathbf{N}_{k,g}^{(m_2)} \left(\log w_g + c_{k,g} \right) - \mathbf{N}_k^{(K)} \log \left(\sum_{g=1}^{G_{m_2}} w_g \exp(c_{k,g}) \right) - \frac{1}{2} \sum_{g=1}^{G_{m_2}} \left(\log |2\pi\sigma_{r_g}^2| + r_g(\sigma_{r_g}^2)^{-1}r_g \right), \quad (25)$$

where $\mathbf{N}_{k,g}^{(m_2)}$ is the total count of component k that is assigned to the g -th grid in the m_2 -th continuous attribute, and $r_g = c_{k,g} - \mathbf{H}\mathbf{m}_{k,g}^p$, $\sigma_{r_g}^2 = \mathbf{H}\mathbf{P}_{k,g}^p\mathbf{H}^T + \sigma_{noise}^2$ is an innovation mean and its variance. The g -th element of the gradient is as follows:

$$\left(\nabla L(\mathbf{c}_k) \right)_g = \mathbf{N}_{k,g}^{(m_2)} - \mathbf{N}_k^{(K)} \frac{w_g \exp(c_{k,g})}{\sum_{g'=1}^{G_{m_2}} w_{g'} \exp(c_{k,g'})} - (\sigma_{r_g}^2)^{-1}r_g. \quad (26)$$

We can estimate \mathbf{c}_k using the L-BFGS method[19] because Eq. (25) has a unique maximum.

4.2 Group Anomaly Detection

We exploit inferred components to calculate an anomaly score of \mathcal{X}^C . Our goal is to detect group anomalies, so we treat a sudden surge in a component's occurrence or an abrupt increase in an attribute's count within a component as a group anomaly. Therefore, we execute the chi-squared goodness-of-fit test.

H₀: The null hypothesis assumes that the average of $\mathbf{N}^{(K)}, \mathbf{N}^{(m_1)}, \mathbf{N}^{(m_2)}$ in the current tensor is the same as the average of them in all previous normal times.

$$\mathbb{E}[\mathbf{N}^{(K)}] = (\mathbf{N}^{(K)} + \mathbf{S}^{(K)}) \frac{\delta_c}{\mathcal{T} + \delta_c}, \quad (27)$$

$$\mathbb{E}[\mathbf{N}^{(m_1)}] = (\mathbf{N}^{(m_1)} + \mathbf{S}^{(m_1)}) \frac{\delta_c}{\mathcal{T} + \delta_c}, \quad (28)$$

$$\mathbb{E}[\mathbf{N}^{(m_2)}] = (\mathbf{N}^{(m_2)} + \mathbf{S}^{(m_2)}) \frac{\delta_c}{\mathcal{T} + \delta_c}, \quad (29)$$

where $\delta_c = \tau_{(t_s+T_c)} - \tau_{t_s}$ is the interval of the current tensor.

H₁: The alternative hypothesis assumes that at least one of $\mathbf{N}^{(K)}, \mathbf{N}^{(m_1)}, \mathbf{N}^{(m_2)}$ contains anomalies, and observed counts show a statistically significant difference from the expected counts, namely, Eq. (27) - (29).

Using the chi-squared statistic, $\chi_m^2(\mathbf{x}, M) = \sum_{m=1}^M (\mathbf{x}_m - \mathbb{E}[\mathbf{x}_m])^2 / \mathbb{E}[\mathbf{x}_m]$, we define the anomaly score as follows:

$$\text{score}(\mathcal{X}^C) = \chi_k^2(\mathbf{N}^{(K)}, K) + \sum_{m_1=1}^{M_1} \sum_{k=1}^K \chi_u^2(\mathbf{N}_{k,\cdot}^{(m_1)}, U_{m_1}) + \sum_{m_2=1}^{M_2} \sum_{k=1}^K \chi_g^2(\mathbf{N}_{k,\cdot}^{(m_2)}, G_{m_2}). \quad (30)$$

LEMMA 4.1 (PROOF IN APPENDIX A.2). $\text{score}(\mathcal{X}^C)$ follows a chi-squared distribution with $K(\sum_{m_1=1}^{M_1} U_{m_1} + \sum_{m_2=1}^{M_2} G_{m_2} - M_1 - M_2 + 1) - 1$ degrees of freedom.

This lemma indicates that we can compute the p-value $P(X > \text{score}(\mathcal{X}^C))$. If the p-value is less than 0.05, we reject the null hypothesis, and thus, \mathcal{X}^C is judged as an anomaly. Otherwise, the null

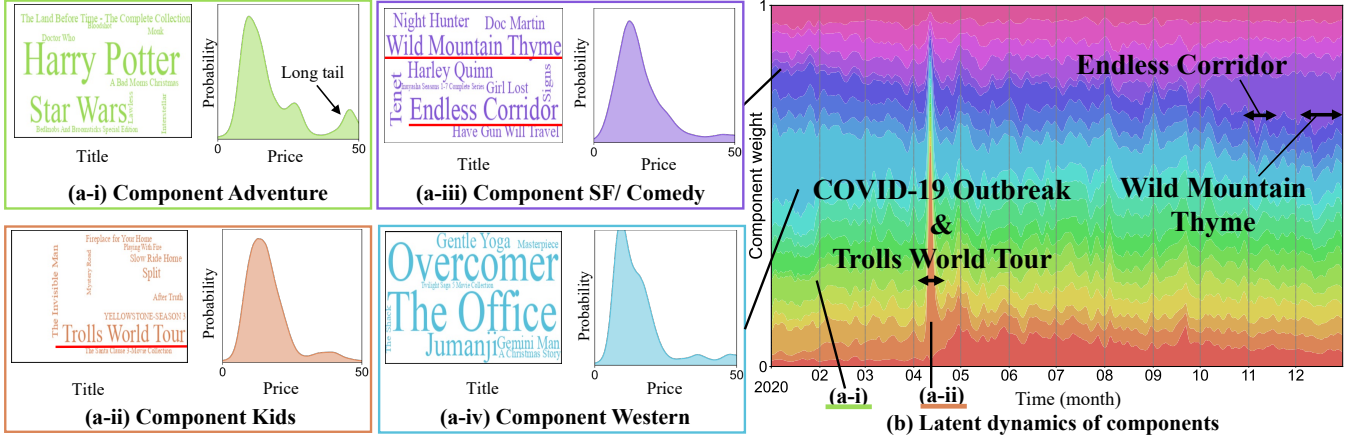


Figure 4: Market analysis of HETEROCOMP in the #6 Amazon Movie&TV dataset. (a) The characteristics of four components (Adventure, Kids, SF/Comedy, Western) in categorical attribute (Title) and continuous attribute (price in US dollars). (b) Component weight exhibit significant changes in relation to the film’s release.

hypothesis cannot be rejected, so we judge \mathcal{X}^C as normal, and add $\delta_c, \mathcal{N}^{(K)}, \{\mathcal{N}^{(m_1)}\}_{m_1=1}^{M_1}, \{\mathcal{N}^{(m_2)}\}_{m_2=1}^{M_2}$ to \mathcal{S} .

Time complexity of HETEROCOMP. Lemma 4.2 indicates that our proposed algorithm requires only constant computational time for the entire data stream length T , thus HETEROCOMP is practical for semi-infinite data streams in terms of execution speed.

LEMMA 4.2 (PROOF IN APPENDIX A.3). *The time complexity HETEROCOMP for the current tensor \mathcal{X}^C is $O(EN_{event}K(M_1 + M_2) + EKT_c p^3 + \sum_{m_1=1}^{M_1} U_{m_1}K + IK \sum_{m_2=1}^{M_2} G_{m_2} p^3)$, where E is the epoch count of component sampling, $N_{event} = \sum_{t=1}^{T_c} N_t$ is the number of records, and I is the L-BFGS iteration count.*

5 Experiments

In this section, we evaluate the performance of HETEROCOMP. The experimental settings are detailed in Appendix B.1. We answer the following questions through the experiments.

- (Q1) *Effectiveness:* How successfully does it discover interpretable summarization of real datasets?
- (Q2) *Accuracy:* How accurately does it detect group anomalies from real datasets?
- (Q3) *Scalability:* How does it scale in terms of computational time?

Datasets. We used five real network traffic/intrusion datasets, namely (#1) *CI’17* [39], (#2) *CCI’18* [13], (#3) *Edge-IIoT* [9], (#4) *DDos2019* [40], (#5) *CUPID* [18], and one user-review dataset, namely (#6) *Amazon Movie&TV* [12].

Baselines. We undertook comparisons with the following competitors for streaming anomaly detection: OneClassSVM [38], iForestASD [6], RRCF [10], ARCUS [51], Mstream [3], MemStream [4], Anograph [5], CubeScope [27], and CyberCscope [26].

5.1 Q1: Effectiveness

We first demonstrate how effectively HETEROCOMP discovers interpretable summarization on real datasets.

User Review Analysis. Fig. 4 shows our mining result for (#6) *Amazon Movie&TV* dataset. First, Fig. 4(a) shows the characteristics of four components, where we manually named them "Adventure",

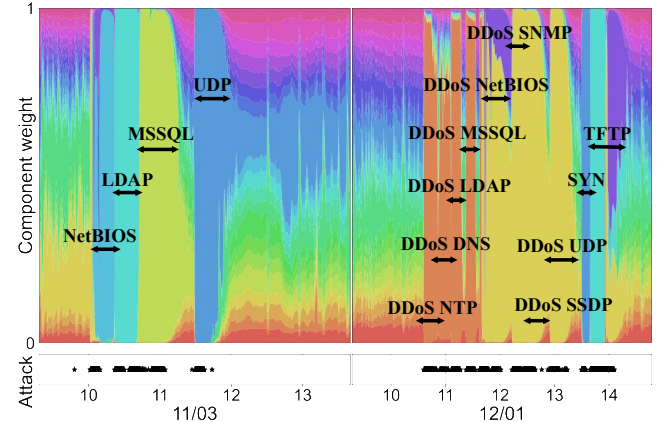


Figure 5: Dynamics of B (above) and attacked time (below) in (#4) DDos2019 dataset.

"Kids", "SF/Comedy", "Western", in title (i.e., A) and price (i.e., C). From the word clouds, Adventure is associated with blockbuster franchises such as Harry Potter and Star Wars. It exhibits a right-skewed price distribution with a high-price tail, whereas Kids (e.g., Trolls World Tour) concentrates in the low-to-mid price range. SF/Comedy (e.g., Endless Corridor, Wild Mountain Thyme, Tenet) and Western (e.g., The Office, Overcomer, Jumanji) films also appear at relatively low prices, with Western having the lowest median price. These observations indicate that each component captures coherent semantics in A while exhibiting distinct regimes in the continuous attribute C. Next, Fig. 4(b) shows the latent dynamics (i.e., B), namely, which components the users are interested in 2020. In April, a spike of component Kids is observed, which is due to the closure of movie theaters caused by the COVID-19 pandemic and Universal’s release of the animation film "Trolls World Tour" via streaming starting on April 10, 2020. Similarly, the release of "Endless Corridor" and "Wild Mountain Thyme" increase the users’ attention to component SF/Comedy.

Table 2: Anomaly detection results. Best results are in bold, and second-best results are underlined (higher is better). The rightmost column shows the average value for each metric.

	#1 CI'17 [39]		#2 CCI'18 [13]		#3 Edge-IoT [9]		#4 DDos2019 [40]		#5 CUPID [18]		Average	
	AUC-ROC	AUC-PR	AUC-ROC	AUC-PR								
OneClassSVM [38]	0.587	0.082	0.594	0.146	0.662	0.601	0.900	0.913	0.467	0.016	0.642	0.352
iForestASD [6]	<u>0.844</u> ± 0.001	<u>0.540</u> ± 0.003	<u>0.781</u> ± 0.001	<u>0.428</u> ± 0.005	0.700 ± 0.009	0.680 ± 0.008	0.881 ± 0.001	0.912 ± 0.001	0.957 ± 0.004	0.608 ± 0.003	0.833	0.634
RRCF [10]	0.877 ± 0.002	0.679 ± 0.004	0.763 ± 0.009	0.337 ± 0.010	0.927 ± 0.002	0.919 ± 0.003	0.896 ± 0.002	0.922 ± 0.001	0.974 ± 0.004	0.705 ± 0.013	0.888	0.712
ARCUS [51]	0.500 ± 0.002	0.028 ± 0.002	0.503 ± 0.004	0.153 ± 0.010	0.501 ± 0.001	0.586 ± 0.178	0.500 ± 0.002	0.280 ± 0.014	0.497 ± 0.008	0.013 ± 0.000	0.500	0.212
MStream [3]	0.905 ± 0.000	0.736 ± 0.000	0.779 ± 0.000	0.363 ± 0.000	0.928 ± 0.000	0.927 ± 0.000	0.899 ± 0.000	0.925 ± 0.000	0.991 ± 0.000	0.734 ± 0.000	0.900	0.737
MemStream [4]	0.893 ± 0.000	0.713 ± 0.000	0.781 ± 0.000	0.366 ± 0.000	<u>0.935</u> ± 0.000	<u>0.935</u> ± 0.000	0.950 ± 0.002	0.956 ± 0.001	0.977 ± 0.000	0.678 ± 0.000	0.907	0.730
Anograph [5]	<u>0.921</u> ± 0.000	<u>0.741</u> ± 0.000	0.776 ± 0.001	0.419 ± 0.005	0.928 ± 0.000	0.920 ± 0.000	<u>0.974</u> ± 0.000	<u>0.970</u> ± 0.000	<u>0.994</u> ± 0.000	0.814 ± 0.001	0.915	0.773
CubeScope [27]	0.921 ± 0.001	0.545 ± 0.003	0.490 ± 0.002	0.123 ± 0.001	0.294 ± 0.004	0.421 ± 0.004	0.684 ± 0.013	0.715 ± 0.010	0.986 ± 0.000	<u>0.872</u> ± 0.004	0.675	0.535
CyberCscope [26]	0.625 ± 0.037	0.302 ± 0.096	0.659 ± 0.090	0.202 ± 0.047	0.771 ± 0.054	0.633 ± 0.056	0.502 ± 0.176	0.574 ± 0.127	0.940 ± 0.034	0.785 ± 0.116	0.699	0.499
HETEROCOMP (ours)	0.990 ± 0.006	0.931 ± 0.037	0.788 ± 0.005	0.644 ± 0.008	0.935 ± 0.003	0.931 ± 0.003	0.963 ± 0.003	0.970 ± 0.002	0.999 ± 0.000	0.959 ± 0.001	0.935	0.887

Cybersecurity systems. As discussed in Section 1, Fig. 1 showed that HETEROCOMP can effectively estimate components with various distributional characteristics and their temporal changes (dynamics). Additionally, Fig. 5 contrasts the temporal variation of the estimated B with the actual time of the cyberattack in the (#4) *DDos2019* dataset. During the attacks, a specific components increases sharply. Please also see the results in (#1) *CI'17* and (#2) *CCI'18* datasets in Appendix B.2.

These results show that HETEROCOMP can capture the interpretable components and their temporal dynamics consistent with external events, such as movie releases or cyber-attacks.

5.2 Q2: Accuracy

We next evaluate the accuracy of HETEROCOMP in terms of group anomaly detection. We defined a current tensor as anomalous if it contains more than one hundred anomalous records. For point-anomaly detection methods, the anomaly score of a current tensor was defined as the sum of the anomaly scores of the records contained within it. Table 2 shows *AUC-ROC* and *AUC-PR* for each method, where a higher value indicates better detection accuracy. All results are averaged over three runs with random seeds. Our proposed method HETEROCOMP achieves the highest average detection accuracy across the datasets, which demonstrates that HETEROCOMP is effective for group anomaly detection. Point-anomaly detection methods (One Class SVM, iForestASD, RRCF, ARCUS) exhibit low performance in detecting group anomalies. MStream and MemStream achieve high detection accuracy, but since they cannot exploit the continuity of timestamps, they suffer from many false positives, resulting in low *AUC-PR*, especially on (#2) *CCI'18* dataset. Although Anograph obtains better performance with (#4) *DDos2019*, it underperforms HETEROCOMP across other datasets because it is a graph-based method and cannot handle multi-aspect data. CubeScope discretizes continuous attributes, and CyberCscope assumes continuous attributes follow only a Gamma distribution, which limit their abilities to represent diverse attribute distributions and degrade detection performance.

5.3 Q3: Scalability

Finally, we verify the computation time of HETEROCOMP. The left part of Fig. 6 shows the average wall clock time of an experiment performed on three datasets, (#1) *CI'17*, (#3) *Edge-IoT*, (#4) *DDos2019*. Although there are slight variations due to differences in the number of records, thanks to the incremental update, HETEROCOMP can maintain stable computational performance independent

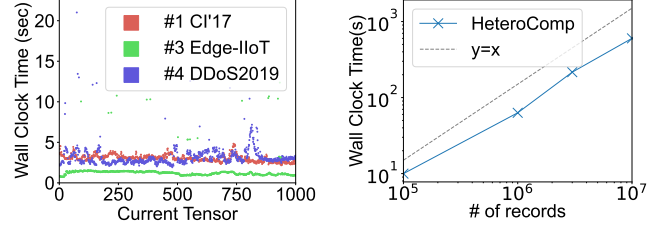


Figure 6: Complexity analysis of HETEROCOMP: (Left) Average wall clock time vs. current tensor. (Right) Wall clock time vs. # of records in X^C . The algorithm scales linearly (i.e., slope = 1 in log-log scale).

of the overall stream length. The right part of Fig. 6 shows the computational time of HETEROCOMP when varying the number of records in X^C . Since HETEROCOMP achieves fast model estimation for $O(N_{event})$ time (as discussed in Lemma 4.2), its computation time is linear with respect to the number of records (i.e., slope = 1 in log-log scale).

6 Conclusion

In this paper, we propose HETEROCOMP, which summarizes heterogeneous tensor streams and detects anomalies in real-time. HETEROCOMP can simultaneously components and their temporal dynamics without restricting to any specific parameterized form of continuous attributes, and immediately detect anomalous behavior based on them. Our approach exhibits all of the following desirable properties that we listed in the introduction. (a) *Effective*: It discovers latent components and their latent dynamics. (b) *Accurate*: Our experiments demonstrated that HETEROCOMP detects group anomalies accurately. (c) *Scalable*: The computational time does not depend on the data stream length.

Acknowledgments

We would like to thank the anonymous referees for their valuable and helpful comments. This work was supported by JSPS KAKENHI Grant-in-Aid for Scientific Research Number JP24KJ1618, JST CREST JPMJCR23M3, JST START JPMJST2553, JST CREST JP-MJCR20C6, JST K Program JPMJKP25Y6, JST COI-NEXT JPMJPF2009, JST COI-NEXT JPMJPF2115, the Future Social Value Co-Creation Project - Osaka University.

References

- [1] Dawon Ahn, Uday Singh Saini, Evangelos E. Papalexakis, and Ali Payani. 2024. Neural Additive Tensor Decomposition for Sparse Tensors. In *Proceedings of the 33rd ACM International Conference on Information and Knowledge Management*

(Boise, ID, USA) (CIKM '24). Association for Computing Machinery, New York, NY, USA, 14–23. doi:10.1145/3627673.3679833

[2] Siddharth Bhatia, Bryan Hooi, Minji Yoon, Kijung Shin, and Christos Faloutsos. 2020. Midas: Microcluster-Based Detector of Anomalies in Edge Streams. In *The Thirty-Fourth AAAI Conference on Artificial Intelligence, AAAI 2020, The Thirty-Second Innovative Applications of Artificial Intelligence Conference, IAAI 2020, The Tenth AAAI Symposium on Educational Advances in Artificial Intelligence, EAAI 2020, New York, NY, USA, February 7-12, 2020*. AAAI Press, New York, NY, USA, 3242–3249. doi:10.1609/AAAI.V34I04.5724

[3] Siddharth Bhatia, Arjit Jain, Pan Li, Ritesh Kumar, and Bryan Hooi. 2021. MStream: Fast Anomaly Detection in Multi-Aspect Streams. In *Proceedings of the Web Conference 2021 (Ljubljana, Slovenia) (WWW '21)*. Association for Computing Machinery, New York, NY, USA, 3371–3382. doi:10.1145/3442381.3450023

[4] Siddharth Bhatia, Arjit Jain, Shivin Srivastava, Kenji Kawaguchi, and Bryan Hooi. 2022. MemStream: Memory-Based Streaming Anomaly Detection. In *Proceedings of the ACM Web Conference 2022 (WWW '22)*. Association for Computing Machinery, New York, NY, USA, 610–621. doi:10.1145/3485447.3512221

[5] Siddharth Bhatia, Mohit Wadhwa, Kenji Kawaguchi, Neil Shah, Philip S. Yu, and Bryan Hooi. 2023. Sketch-Based Anomaly Detection in Streaming Graphs. In *Proceedings of the 29th ACM SIGKDD Conference on Knowledge Discovery and Data Mining (Long Beach, CA, USA) (KDD '23)*. Association for Computing Machinery, New York, NY, USA, 93–104. doi:10.1145/3580305.3599504

[6] Zhiqiu Ding and Minrui Fei. 2013. An Anomaly Detection Approach Based on Isolation Forest Algorithm for Streaming Data using Sliding Window. *IFAC Proceedings Volumes* 46, 20 (2013), 12–17. doi:10.3182/20130902-3-CN-3020.00044 3rd IFAC Conference on Intelligent Control and Automation Science ICONS 2013.

[7] Yishuai Du, Yimin Zheng, Kuang-chih Lee, and Shandian Zhe. 2018. Probabilistic Streaming Tensor Decomposition. In *2018 IEEE International Conference on Data Mining (ICDM)*. IEEE Computer Society, Singapore, Singapore, 99–108. doi:10.1109/ICDM.2018.00025

[8] Ocheme Anthony Ekle and William Eberle. 2024. Anomaly Detection in Dynamic Graphs: A Comprehensive Survey. *ACM Trans. Knowl. Discov. Data* 18, 8, Article 192 (July 2024), 44 pages. doi:10.1145/3669906

[9] Mohamed Amine Ferrag, Othmane Frihi, Djallel Hamouda, Leandros Maglaras, and Helge Janicke. 2022. Edge-IoTSet: A New Comprehensive Realistic Cyber Security Dataset of IoT and IIoT Applications: Centralized and Federated Learning. doi:10.21227/mbe1-1h68

[10] Sudipto Guha, Nina Mishra, Gourav Roy, and Okke Schrijvers. 2016. Robust Random Cut Forest Based Anomaly Detection on Streams. In *Proceedings of The 33rd International Conference on Machine Learning (Proceedings of Machine Learning Research, Vol. 48)*. Maria Florina Balcan and Kilian Q. Weinberger (Eds.). PMLR, New York, New York, USA, 2712–2721. <https://proceedings.mlr.press/v48/guha16.html>

[11] Bryan Hooi, Kijung Shin, Shenghua Liu, and Christos Faloutsos. 2019. SMF: Drift-Aware Matrix Factorization with Seasonal Patterns. In *Proceedings of the 2019 SIAM International Conference on Data Mining (SDM)*. Society for Industrial and Applied Mathematics, Calgary, Alberta, Canada, 621–629. arXiv:<https://epubs.siam.org/doi/pdf/10.1137/1.9781611975673.70> doi:10.1137/1.9781611975673.70

[12] Yupeng Hou, Jiacheng Li, Zhankui He, An Yan, Xiusi Chen, and Julian McAuley. 2024. Bridging Language and Items for Retrieval and Recommendation. <https://amazon-reviews-2023.github.io/>

[13] Sharafaldin Iman, Lashkari Arash, Habibi, and Ghorbani Ali, A. 2018. CSE-CIC-IDS2018 on AWS. <https://www.unb.ca/cic/datasets/ids-2018.html>

[14] Meng Jiang, Alex Beutel, Peng Cui, Bryan Hooi, Shiqiang Yang, and Christos Faloutsos. 2015. A General Suspiciousness Metric for Dense Blocks in Multimodal Data. In *Proceedings of the 2015 IEEE International Conference on Data Mining (ICDM) (ICDM '15)*. IEEE Computer Society, USA, 781–786. doi:10.1109/ICDM.2015.61

[15] Koki Kawabata, Siddharth Bhatia, Rui Liu, Mohit Wadhwa, and Bryan Hooi. 2021. SSMF: Shifting Seasonal Matrix Factorization. In *Advances in Neural Information Processing Systems 34*, Vol. 34. Curran Associates, Inc., 3863–3873.

[16] Tamara G. Kolda and Brett W. Bader. 2009. Tensor Decompositions and Applications. *SIAM Rev.* 51, 3 (2009), 455–500. arXiv:<https://doi.org/10.1137/07070111X> doi:10.1137/07070111X

[17] Taehyung Kwon, Inkyu Park, Dongjin Lee, and Kijung Shin. 2021. SliceNSTitch: Continuous CP Decomposition of Sparse Tensor Streams. In *2021 IEEE 37th International Conference on Data Engineering (ICDE)*, Vol. 1. IEEE Computer Society, Los Alamitos, CA, USA, 816–827. doi:10.1109/ICDE51399.2021.00076

[18] Heather Lawrence, Uchenna Ezeobi, Orly Tauli, Jacob Nosal, Owen Redwood, Yanyan Zhuang, and Gedare Bloom. 2022. CUPID: A labeled dataset with Pentesting for evaluation of network intrusion detection. *Journal of Systems Architecture* 129 (2022), 102621. doi:10.1016/j.sysarc.2022.102621

[19] {Dong C} Liu and Jorge Nocedal. 1989. On the limited memory BFGS method for large scale optimization. *Mathematical Programming* 45, 1-3 (Aug. 1989), 503–528. doi:10.1007/BF01589116

[20] Lisa Liu, Gints Engelen, Timothy Lynam, Daryl Essam, and Wouter Joosen. 2022. Error Prevalence in NIDS datasets: A Case Study on CIC-IDS-2017 and CSE-CIC-IDS-2018. *2022 IEEE Conference on Communications and Network Security (CNS)* 00 (2022), 254–262.

[21] Jie Lu, Anjin Liu, Fan Dong, Feng Gu, João Gama, and Guangquan Zhang. 2017. Learning under Concept Drift: A Review. *IEEE Transactions on Knowledge and Data Engineering* 31, 12 (2017), 2346–2363. arXiv:2004.05785

[22] Emaad Manzoor, Hemank Lamba, and Leman Akoglu. 2018. xStream: Outlier Detection in Feature-Evolving Data Streams. *Proceedings of the 24th ACM SIGKDD International Conference on Knowledge Discovery & Data Mining* (2018), 1963–1972.

[23] Yasuko Matsubara, Yasushi Sakurai, Christos Faloutsos, Tomoharu Iwata, and Masatoshi Yoshikawa. 2012. Fast mining and forecasting of complex time-stamped events. In *Proceedings of the 18th ACM SIGKDD International Conference on Knowledge Discovery and Data Mining (Beijing, China) (KDD '12)*. Association for Computing Machinery, New York, NY, USA, 271–279. doi:10.1145/2339530.2339577

[24] Jacob Montiel, Max Halford, Saulo Martiello Mastelini, Geoffrey Bolmier, Raphael Soury, Robin Vaysse, Adil Zouitine, Heitor Murilo Gomes, Jesse Read, Taleb Abdessalem, and Albert Bifet. 2021. River: machine learning for streaming data in Python. *Journal of Machine Learning Research* 22, 110 (2021), 1–8. <http://jmlr.org/papers/v22/20-1380.html>

[25] Gyoung S Na, Donghyun Kim, and Hwanjo Yu. 2018. DILOF: Effective and Memory Efficient Local Outlier Detection in Data Streams. *Proceedings of the 24th ACM SIGKDD International Conference on Knowledge Discovery and Data Mining* (2018), 1993–2002.

[26] Kota Nakamura, Koki Kawabata, Shungo Tanaka, Yasuko Matsubara, and Yasushi Sakurai. 2025. CyberCScope: Mining Skewed Tensor Streams and Online Anomaly Detection in Cybersecurity Systems. In *Companion Proceedings of the ACM on Web Conference 2025 (Sydney NSW, Australia) (WWW '25)*. Association for Computing Machinery, New York, NY, USA, 1214–1218. doi:10.1145/3701716.3715476

[27] Kota Nakamura, Yasuko Matsubara, Koki Kawabata, Yuhei Umeda, Yuichiro Wada, and Yasushi Sakurai. 2023. Fast and Multi-aspect Mining of Complex Time-stamped Event Streams. In *Proceedings of the ACM Web Conference 2023 (Austin, TX, USA) (WWW '23)*. Association for Computing Machinery, New York, NY, USA, 1638–1649. doi:10.1145/3543507.3583370

[28] Alfredo Názařábal, Pablo M. Olmos, Zoubin Ghahramani, and Isabel Valera. 2020. Handling incomplete heterogeneous data using VAEs. *Pattern Recognition* 107 (2020), 107501. doi:10.1016/j.patcog.2020.107501

[29] Maya Okawa, Tomoharu Iwata, Takeshi Kurashima, Yusuke Tanaka, Hiroyuki Toda, and Naonori Ueda. 2019. Deep Mixture Point Processes: Spatio-temporal Event Prediction with Rich Contextual Information. In *Proceedings of the 25th ACM SIGKDD International Conference on Knowledge Discovery & Data Mining (Anchorage, AK, USA) (KDD '19)*. Association for Computing Machinery, New York, NY, USA, 373–383. doi:10.1145/3292500.3330937

[30] Dragoljub Pokrajac, Aleksandar Lazarevic, and Longin Jan Latecki. 2007. Incremental Local Outlier Detection for Data Streams. *2007 IEEE Symposium on Computational Intelligence and Data Mining* (2007), 504–515.

[31] Nicholas G. Polson, James G. Scott, and Jesse Windle. 2013. Bayesian Inference for Logistic Models Using Pólya–Gamma Latent Variables. *J. Amer. Statist. Assoc.* 108, 504 (2013), 1339–1349. arXiv:<https://doi.org/10.1080/01621459.2013.829001> doi:10.1080/01621459.2013.829001

[32] Ian Porteous, David Newman, Alexander Ihler, Arthur Asuncion, Padhraic Smyth, and Max Welling. 2008. Fast collapsed gibbs sampling for latent dirichlet allocation. In *Proceedings of the 14th ACM SIGKDD International Conference on Knowledge Discovery and Data Mining (Las Vegas, Nevada, USA) (KDD '08)*. Association for Computing Machinery, New York, NY, USA, 569–577. doi:10.1145/1401890.1401960

[33] Carl Edward Rasmussen and Christopher K. I. Williams. 2005. *Gaussian Processes for Machine Learning*. The MIT Press, Cambridge, MA. doi:10.7551/mitpress/3206.001.0001

[34] Danilo Jimenez Rezende and Shakir Mohamed. 2015. Variational inference with normalizing flows. In *Proceedings of the 32nd International Conference on International Conference on Machine Learning - Volume 37* (Lille, France) (ICML '15). JMLR.org, 1530–1538.

[35] Jaakko Riihimäki and Aki Vehtari. 2012. Laplace Approximation for Logistic Gaussian Process Density Estimation and Regression. *Bayesian Analysis* 9 (11 2012). doi:10.1214/14-BA872

[36] Mahsa Salehi, Christopher Leckie, James C. Bezdek, Tharshan Vaithianathan, and Xuyun Zhang. 2016. Fast Memory Efficient Local Outlier Detection in Data Streams. *IEEE Transactions on Knowledge and Data Engineering* 28, 12 (2016), 3246–3260. doi:10.1109/TKDE.2016.2597833

[37] Aaron Schein, John Paisley, David M. Blei, and Hanna Wallach. 2015. Bayesian Poisson Tensor Factorization for Inferring Multilateral Relations from Sparse Dyadic Event Counts. In *Proceedings of the 21th ACM SIGKDD International Conference on Knowledge Discovery and Data Mining (Sydney, NSW, Australia) (KDD '15)*. Association for Computing Machinery, New York, NY, USA, 1045–1054. doi:10.1145/2783258.2783414

[38] Bernhard Schölkopf, Robert C Williamson, Alex Smola, John Shawe-Taylor, and John Platt. 1999. Support Vector Method for Novelty Detection. In *Advances in Neural Information Processing Systems*, S. Solla, T. Leen, and K. Müller (Eds.),

Vol. 12. MIT Press, Denver, Colorado, USA. https://proceedings.neurips.cc/paper_files/paper/1999/file/8725fb77f25776ffa9076e44fcfd776-Paper.pdf

[39] Iman Sharafaldin, Arash Habibi Lashkari, and Ali A. Ghorbani. 2018. Toward Generating a New Intrusion Detection Dataset and Intrusion Traffic Characterization. In *Proceedings of the 4th International Conference on Information Systems Security and Privacy, ICISPP 2018, Funchal, Madeira - Portugal, January 22–24, 2018*, Paolo Mori, Steven Furnell, and Olivier Camp (Eds.). SciTePress, Madeira, Portugal, 108–116. doi:10.5220/0006639801080116

[40] Iman Sharafaldin, Arash Habibi Lashkari, Saqib Hakak, and Ali A. Ghorbani. 2019. Developing Realistic Distributed Denial of Service (DDoS) Attack Dataset and Taxonomy. In *2019 International Carnahan Conference on Security Technology (ICCS)*. IEEE, Chennai, India, 1–8. doi:10.1109/CCST.2019.8888419

[41] Kijung Shin, Bryan Hooi, Jisu Kim, and Christos Faloutsos. 2017. DenseAlert: Incremental Dense-Subtensor Detection in Tensor Streams. In *Proceedings of the 23rd ACM SIGKDD International Conference on Knowledge Discovery and Data Mining* (Halifax, NS, Canada) (KDD '17). Association for Computing Machinery, New York, NY, USA, 1057–1066. doi:10.1145/3097983.3098087

[42] Shaden Smith, Kejun Huang, Nicholas D. Sidiropoulos, and George Karypis. 2018. *Streaming Tensor Factorization for Infinite Data Sources*. 81–89. arXiv:<https://pubs.siam.org/doi/pdf/10.1137/1.9781611975321.10> doi:10.1137/1.9781611975321.10

[43] Simo Särkkä and Arno Solin. 2019. *Applied Stochastic Differential Equations*. Cambridge University Press.

[44] Conor Tillinghast and Shandian Zhe. 2021. Nonparametric Decomposition of Sparse Tensors. In *Proceedings of the 38th International Conference on Machine Learning (Proceedings of Machine Learning Research, Vol. 139)*, Marina Meila and Tong Zhang (Eds.). PMLR, 10301–10311. <https://proceedings.mlr.press/v139/tillinghast21a.html>

[45] VictorHoffmann1. 2025. Implementation of Sketch-Based Anomaly Detection in Streaming Graphs paper. <https://github.com/VictorHoffmann1/AnoGraph-for-River-API> GitHub repository.

[46] Zheng Wang, Xinqi Chu, and Shandian Zhe. 2020. Self-Modulating Nonparametric Event-Tensor Factorization. In *Proceedings of the 37th International Conference on Machine Learning (Proceedings of Machine Learning Research, Vol. 119)*, Hal Daumé III and Aarti Singh (Eds.). PMLR, 9857–9867. <https://proceedings.mlr.press/v119/wang20d.html>

[47] Zheng Wang, Yiming Xu, Conor Tillinghast, Shibo Li, Akil Narayan, and Shandian Zhe. 2022. Nonparametric Embeddings of Sparse High-Order Interaction Events. In *Proceedings of the 39th International Conference on Machine Learning (Proceedings of Machine Learning Research, Vol. 162)*, Kamalika Chaudhuri, Stefanie Jegelka, Le Song, Csaba Szepesvari, Gang Niu, and Sivan Sabato (Eds.). PMLR, Baltimore, Maryland, USA, 23237–23253. <https://proceedings.mlr.press/v162/wang22ah.html>

[48] Lei Xu, María Skoularidou, Alfredo Cuesta-Infante, and Kalyan Veeramachaneni. 2019. *Modeling tabular data using conditional GAN*. Curran Associates Inc, Red Hook, NY, USA.

[49] Selim F. Yilmaz and Suleyman S. Kozat. 2025. PySAD: A Streaming Anomaly Detection Framework in Python. arXiv:2009.02572 [cs.LG] <https://arxiv.org/abs/2009.02572>

[50] Susik Yoon, Jae-Gil Lee, and Byung Suk Lee. 2019. NETS: extremely fast outlier detection from a data stream via set-based processing. *Proc. VLDB Endow.* 12, 11 (July 2019), 1303–1315. doi:10.14778/3342263.3342269

[51] Susik Yoon, Younghun Lee, Jae-Gil Lee, and Byung Suk Lee. 2022. Adaptive Model Pooling for Online Deep Anomaly Detection from a Complex Evolving Data Stream. In *Proceedings of the 28th ACM SIGKDD Conference on Knowledge Discovery and Data Mining* (Washington DC, USA) (KDD '22). Association for Computing Machinery, New York, NY, USA, 2347–2357. doi:10.1145/3534678.3539348

[52] Susik Yoon, Yooju Shin, Jae-Gil Lee, and Byung Suk Lee. 2021. Multiple Dynamic Outlier-Detection from a Data Stream by Exploiting Duality of Data and Queries. In *Proceedings of the 2021 International Conference on Management of Data (SIGMOD '21)*. Association for Computing Machinery, New York, NY, USA, 2063–2075. doi:10.1145/3448016.3452810

[53] Jiabao Zhang, Shenghua Liu, Wenting Hou, Siddharth Bhatia, Huawei Shen, Wenjian Yu, and Xueqi Cheng. 2021. AugSplicing: Synchronized Behavior Detection in Streaming Tensors. *Proceedings of the AAAI Conference on Artificial Intelligence* 35, 5 (2021), 4653–4661. doi:10.1609/aaai.v35i5.16595

[54] Shandian Zhe and Yishuai Du. 2018. Stochastic Nonparametric Event-Tensor Decomposition. In *Advances in Neural Information Processing Systems*, S. Bengio, H. Wallach, H. Larochelle, K. Grauman, N. Cesa-Bianchi, and R. Garnett (Eds.), Vol. 31. Curran Associates, Inc. https://proceedings.neurips.cc/paper_files/paper/2018/file/61f2585b0ebcf1f532c4d1ec9a7d51aa-Paper.pdf

[55] Shuo Zhou, Sarah Erfani, and James Bailey. 2018. Online CP Decomposition for Sparse Tensors. In *2018 IEEE International Conference on Data Mining (ICDM)*. IEEE Computer Society, Los Alamitos, CA, USA, 1458–1463. doi:10.1109/ICDM.2018.00202

[56] Bo Zong, Qi Song, Martin Renqiang Min, Wei Cheng, Cristian Lumezanu, Daeki Cho, and Haifeng Chen. 2018. Deep Autoencoding Gaussian Mixture Model

for Unsupervised Anomaly Detection. In *International Conference on Learning Representations*.

Appendix

A Proposed model

A.1 Symbols

The main symbols we use in this paper are defined in Table 3.

Table 3: Symbol and its definition.

Symbol	Definition
X	Whole event tensor stream, i.e., $X \in \mathbb{N}^{T \times \prod_{m_1=1}^{M_1} U_{m_1} \times \prod_{m_2=1}^{M_2} \mathbb{R}}$.
X^C	Current tensor, i.e., $X^C \in \mathbb{N}^{T_c \times \prod_{m_1=1}^{M_1} U_{m_1} \times \prod_{m_2=1}^{M_2} \mathbb{R}}$.
M_1	Number of categorical attributes in tensor.
M_2	Number of continuous attributes in tensor.
U_1, \dots, U_{M_1}	Number of unique values in categorical attribute.
T_c	Number of unique timestamps in current tensor.
$\tau_{(t_s+1)}, \dots, \tau_{(t_s+T_c)}$	Timestamps in X^C .
δ_c	Time interval of X^C , i.e., $\delta_c = \tau_{(t_s+T_c)} - \tau_{t_s}$.
K	Number of components.
$\mathbf{A}^{(m_1)} \in \mathbb{R}^{K \times U_{m_1}}$	Parameters of m_1 -th categorical attribute.
$\mathbf{C}^{(m_2)} \in \mathbb{R}^{K \times G_{m_2}}$	Parameters of m_2 -th continuous attribute.
$\mathbf{B} \in \mathbb{R}^{K \times T_c}$	Latent dynamics of components.
$\hat{\mathbf{A}}^{(m_1)}, \hat{\mathbf{B}}, \hat{\mathbf{C}}^{(m_2)}$	$\mathbf{A}^{(m_1)}, \mathbf{B}, \mathbf{C}^{(m_2)}$ estimated at the previous tensor.
G_1, \dots, G_{M_2}	Number of grids in continuous attribute.
$\Delta_1^{(m_2)}, \dots, \Delta_{G_{m_2}}^{(m_2)}$	Grids of cmode.
$\kappa_{\mathbf{B}}, \kappa_{\mathbf{C}}$	Kernel covariance function of \mathbf{B}, \mathbf{C} .
$N_t \in \mathbb{N}$	Number of records at time t_t .
$\mathbf{N}^{(K)} \in \mathbb{N}^K$	Component count vector of records in X^C .
$N_{t,k} \in \mathbb{N}$	Number of records assigned to component k at time t_t .
$\mathbf{N}^{(m_1)} \in \mathbb{N}^{K \times U_{m_1}}$	Component-unit count matrix for m_1 -th categorical attribute in X^C .
$\mathbf{N}^{(m_2)} \in \mathbb{N}^{K \times G_{m_2}}$	Component-grid count matrix for m_2 -th continuous attribute in X^C .
Θ	Model Parameters set, defined in Definition 1.
\mathcal{S}	Stream Statistics, defined in Definition 2.
score(X^C)	Anomaly score of X^C .

A.2 Proof of Lemma 4.1

PROOF. $\chi_k^2(\mathbf{N}^{(K)}, K)$ follows a chi-squared distribution with $K-1$ degrees of freedom. After the component is assigned, $\chi_u^2(\mathbf{N}_{k,\cdot}^{(m_1)}, U_{m_1})$ are independently distributed for each component, each adhering to a chi-squared distribution with $U_{m_1}-1$ degrees of freedom. Similarly, after the component is assigned, $\chi_g^2(\mathbf{N}_{k,\cdot}^{(m_2)}, G_{m_2})$ are independently distributed for each component, each adhering to a chi-squared distribution with $G_{m_2}-1$ degrees of freedom. The sum of independent chi-squared random variables follows a chi-squared distribution with degrees of freedom equal to the sum of their individual degrees of freedom. Therefore, score(X^C) follows a chi-squared distribution with $K(\sum_{m_1=1}^{M_1} U_{m_1} + \sum_{m_2=1}^{M_2} G_{m_2} - M_1 - M_2 + 1) - 1$ degrees of freedom. \square

A.3 Proof of Lemma 4.2

PROOF. Derive the time complexity for each element. For each iteration, sampling a component requires $O(N_{even} K(M_1 + M_2))$ because we need $O(K(M_1 + M_2))$ to compute Equation (6) for each event. And estimation of \mathbf{B} requires $O(KT_c p^3)$ because the computation of Equation (9, 10) requires $O(T_c)$, and Forward-Backward algorithm (16)-(23) requires $O(T_c p^3)$ for each component.

Estimation of \mathbf{A} requires $O(U_{m_1} K)$ to compute (26), so the total cost is $O(\sum_{m_1=1}^{M_1} U_{m_1} K)$.

Table 4: Dataset description. Here, ‘fwd’ and ‘bwd’ denote ‘forward’ and ‘backward,’ respectively.

Dataset	Categorical	M_1	Continuous	M_2
#1 CI'17 [39]	(Src/ Dst) IP address Protocol Dst port	4	Flow duration Total length of (fwd /bwd) packet (Fwd /Bwd) header length Flow IAT mean	6
#2 CCI'18 [13]	"	4	"	6
#3 Edge-IIoT [9]	(Src/ Dst) IP address (Src/ Dst) port TCP flag Protocol	6	TCP length	1
#4 DDoS2019 [40]	(Src/ Dst) IP address Protocol	3	Flow duration Total length of fwd packet Fwd header length ACK flag count Flow bytes/s Flow packets/s	6
#5 CUPID [18]	(Src/ Dst) IP address (Src/ Dst) Pport Protocol	5	Flow duration Total length of fwd packet Bwd header length Flow IAT mean Flow bytes/s Flow packets/s Minimum fwd seg size	7
#6 Amazon Movie&TV [12]	Title Category flag(Action, Adventure, Anime, Arts, Cerebral Christmas, Classical, Comedy, Documentary, Fantasy, Fitness, Horror, Kids, Military, Music, Musicals, Mystery, Religion, Romance, SF, Thriller, Westerns)	23	Price	1

In the estimation of \mathbf{C} , the computation of the gradient (26) requires $O(G_{m_2}p^3)$ for the Forward-Backward algorithm (16)–(23). We repeat this computation for each iteration, for each component, and for each continuous attribute, so the total cost is $O(IK \sum_{m_2=1}^{M_2} G_{m_2}p^3)$.

In the anomaly detection, the computation of Equation (30) requires $O(K + \sum_{m_1=1}^{M_1} U_{m_1}K + \sum_{m_2=1}^{M_2} G_{m_2}K)$.

Aggregating these, the total computational complexity is $O(E N_{event}K(M_1 + M_2) + EKT_c p^3 + \sum_{m_1=1}^{M_1} U_{m_1}K + IK \sum_{m_2=1}^{M_2} G_{m_2}p^3)$. \square

B Experimental Evaluation

B.1 Experimental Setup

In this section, we describe the experimental setup in detail. We conducted all our experiments on an Intel Xeon Gold 6444Y 3.6GHz quad core CPU with 768GB of memory and running Linux.

Hyperparameter. We use the Matern-3/2 kernel function as a κ_B, κ_C . We set the number of components K to 20. We set the number of grids $G = 300$ for all continuous attributes, and epoch count $E = 30$. We set the current tensor size T_c to 30 for (#1) CI'17, (#2) CCI'18, (#3) Edge-IIoT, (#4) DDoS2019, (#5) CUPID datasets, and 14 for (#6) Amazon Movie&TV dataset.

Datasets. Table 4 summarizes the features employed in the experiments.

- (#1) CI'17 [39]: It consists of up to 18 million event logs, in which various types of intrusions occur over time. Normal user behavior is executed through scripts. The data set contains a wide range of attack types like SSH brute force, heartbleed, botnet, DoS, DDoS, web and infiltration attacks. A previous study [20] reported errors in this dataset and released improved versions ⁴, which we used throughout the experiments.

- (#2) CCI'18 [13]: It includes seven different attack scenarios: Brute-force, Heartbleed, Botnet, DoS, DDoS, Web attacks, and infiltration of the network from inside. The attacking infrastructure includes 50 machines and the victim organization has 5 departments and includes 420 machines and 30 servers. The dataset includes the captures network traffic and system logs of each machine, along with 80 features extracted from the captured traffic using CICFlowMeter-V3. A previous study [20] reported errors in this dataset and released improved versions ⁵, which we used throughout the experiments.

- (#3) Edge-IIoT [9]: It is a new comprehensive cybersecurity dataset for IoT and IIoT applications, designed for intrusion detection systems⁶.
- (#4) DDoS2019 [40]: It is a realistic and comprehensive dataset for evaluating Distributed Denial of Service (DDoS) attack detection systems, as existing datasets have significant shortcomings ⁷.
- (#5) CUPID [18]: It emulates a small physical network with several virtualized systems ⁸. Its main objective is to provide both scripted and human-generated traffic produced by professional penetration testers, allowing researchers to investigate the differences between the two.

⁴<https://intrusion-detection.distrinet-research.be/CNS2022/CICIDS2017.html>

⁵<https://intrusion-detection.distrinet-research.be/CNS2022/CSECICIDS2018.html>

⁶<https://iee-dataport.org/documents/edge-iiotset-new-comprehensive-realistic-cyber-security-dataset-iot-and-iiot-applications>

⁷<https://www.unb.ca/cic/datasets/ddos-2019.html>

⁸<https://www.kaggle.com/datasets/dhoogla/cupid-2022>

- (#6) Amazon Movie&TV [12]: It is a large-scale Amazon Reviews dataset, collected in 2023 by McAuley Lab ⁹.

Baselines. The details of the baselines we used throughout our extensive experiments are summarized as follows:

- OneClassSVM(One Class Solid Vector Machine) [38]: It is a classification principled data stream anomaly detection algorithm. We set an upper bound on the fraction to 0.1, and the learning rate to 0.01.
- iForestASD [6]: An Anomaly Detection Approach Based on Isolation Forest Algorithm for Streaming Data using Sliding Window. Following [4], we set the window size to 2048 and the number of estimators to 100.
- RRCF(Robust Random Cut Forest) [10]: Isolation Forest-based method designed for the high-dimensional data anomaly detection problem. Following [4], we set the number of trees to 4, and shingle size to 4, and size of tree to 256.
- ARCUS [51]: A deep online anomaly detection framework, which uses an adaptive model pool to manage multiple classification models to handle multiple temporal concept drifts. We use DAGMM [56] as instances of ARCUS. Following the original paper, we set the batch size to 512, the learning rate to 0.0001, the number of layers in AE to 3, the latent dimensionality of AE to 24, and the minimum batch size to 32.
- MStream [3]: A streaming multi-aspect data anomaly detection framework using locality sensitive hashing. We set the temporal decay factor to $\alpha = 0.5$.
- MemStream [4]: Streaming approach using a denoising AutoEncoder and a memory module. We set the memory size $N = 64$ and the threshold for concept drift $\beta = 0.01$.

⁹<https://amazon-reviews-2023.github.io/>

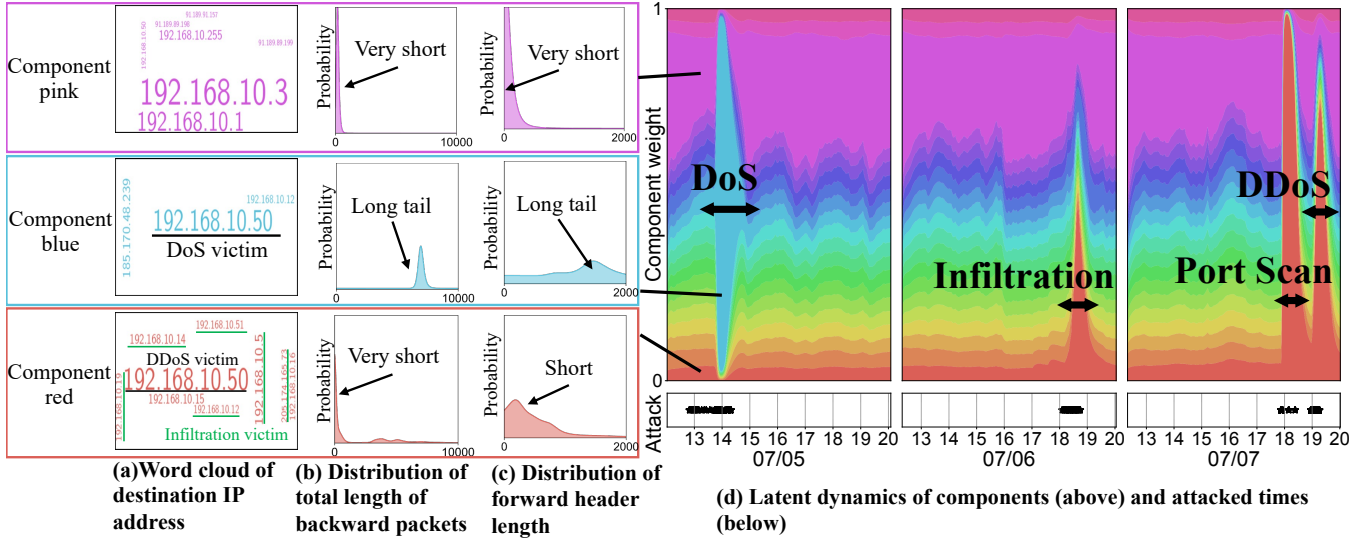


Figure 7: Modeling power of HETEROCOMP over (#1) CI'17 dataset. Our proposed method can find the hidden components which represents different characteristics in both (a) categorical attribute and (b) (c)continuous attributes, and (d) component weight exhibit significant changes when cyber-attacks occurs.

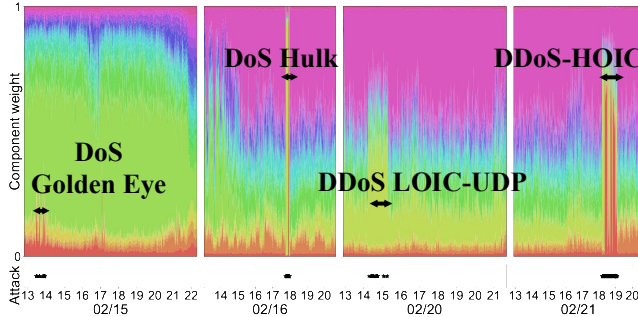


Figure 8: Dynamics of B in (#2) CCI'18. The area of each color represents the component assignment probability at each time.

- Anograph [5]: Graph based streaming anomaly detection method. Following the original paper, we set the number of buckets to 32, edge thresholds to 100, and time window to 60.
- CubeScope [27]: An online tensor factorization method based on probabilistic generative models. We set component size to $K = 48$, as used in [26].
- CyberCScope [26]: A tensor decomposition method which detects time-varying anomaly patterns while distinguishing between categorical attributes and continuous attributes. We set component size to $K = 48$, as used in the original paper.

We used open-sourced implementations of ARCUS [51], MStream [3], MemStream [4], CubeScope [27], CyberCScope [26], provided by the authors. For iForestASD [6] and RRCF [10], we use the open-source library PySAD [49] implementation. We also used the open-source implementation of OneClassSVM [38] in the river library [24]. For Anograph [5], we use the open-source implementation [45] because the original code is implemented in C.

B.2 Effectiveness

We also demonstrate how effectively HETEROCOMP works on datasets different from the ones presented in Section 5.1. Fig. 7 shows the analysis of (#1) CI'17 dataset. Fig. 7(a)(b)(c) shows the characteristics of three components pink, blue, red. First, Fig. 7(a) shows the word clouds of destination IP address attribute (i.e., A). A larger size in the word cloud denote a stronger relationship with the component. Component pink contains records sent to IP address 192.168.10.3 and 192.168.10.3, while Component blue consists of records sent to 192.168.10.50, the victim of the DoS attack. Component red consists of the victims of the Infiltration attack (green underlined) and the victim of DDoS attack (i.e., 192.168.10.50). Next, Fig. 7(b) and Fig. 7(c) show the probability density of the total length of backward packets and the probability distribution of the forward header length, respectively (i.e., C). In Fig. 7(b), component pink and red follow exponential-like distributions, whereas component blue shows a long-tailed distribution, indicating that records in pink and red have shorter total backward packet lengths, while those in blue tend to have longer ones. These results show that HETEROCOMP can flexibly represent various distributions of continuous attributes according to the data. Fig. 7 (d) visualizes the latent dynamics of components (i.e., B) in the (#1) CI'17 dataset. During DoS attacks, component blue dominates, whereas component red increases sharply during Infiltration and Port Scan attacks.

Similarly, Fig. 8 visualizes the latent dynamics of components (i.e., B) and attacked times in the (#2) CCI'18 dataset. The proportions of components red and green increased sharply during periods of cyber-attacks (e.g., DoS Golden Eye, DoS Hulk, DDoS LOIC-UDP, DDoS-HOIC).

These results show that HETEROCOMP can capture the interpretable components in both categorical and continuous attributes, and their temporal dynamics consistent with external events, such as cyber-attacks.